Supporting Information

Suppressing Thermal Evaporation-Induced Iodine Outgassing and Interfacial Degradation in Perovskite Solar Cells

Danqing Ma[1], Kanak Kanti Bhowmik[1], Lin Zhu[1], Anton Ievlev[2], Yongtao Liu[2], Lianfeng Zhao[1,]*

[1]Holcombe Department of Electrical and Computer Engineering, Clemson University, Clemson, South Carolina 29634, United States

[2]Center for Nanophase Materials Sciences, Oak Ridge National Laboratory, Oak Ridge, TN, 37830, USA

[*]Email: Lianfez@clemson.edu

Table S1. Fitting parameters from the tri-exponential fit of the mapping-derived overall PL decays for pristine perovskite films before and after chlorobenzene washing.

Sample	A_1	τ_1	A_2	τ_2	A_3	τ_3	τ_{avg}
Before CB Wash	0.67091	1.224 ns	0.28563	7.51 ns	0.10246	40.19 ns	25.78 ns
After CB Wash	0.58355	1.041 ns	0.32905	6.590 ns	0.12339	36.114 ns	24.32 ns

Table S2. Photovoltaic parameters of pristine devices before and after vacuum or thermal-radiation exposure.

Sample	*J*sc (mA/cm^2)	*V*oc (V)	FF (%)	PCE (%)
Pristine	23.08	1.087	77.54	19.44
30mins Vacuum	22.83	1.083	76.77	18.97
30mins Radiation	23.03	1.034	72.14	17.17

Table S3. Fitting parameters from the tri-exponential fit of the TRPL decay curves for different concentrations of $FA_{0.90}MA_{0.05}Cs_{0.05}PbI_3$ films before and after thermal radiation exposure.

Time	Pristine film- 1.5 M	Pristine film w/ Radiation- 1.5 M	Pristine film- 1.25 M	Pristine film w/ Radiation- 1.25 M	Pristine film- 1 M	Pristine film w/ Radiation- 1 M
A_1	0.63138	0.61984	0.63334	0.59906	0.57455	0.65064
τ_1	1.049 ns	0.951 ns	1.2289 ns	0.930 ns	1.103 ns	1.232 ns
A_2	0.28797	0.26507	0.31167	0.31941	0.33087	0.28891
τ_2	6.973 ns	6.177 ns	6.748 ns	5.408 ns	5.807 ns	5.122 ns
A_3	0.10808	0.08575	0.09626	0.13663	0.11387	0.10591
τ_3	43.314 ns	36.600 ns	38.017 ns	23.148 ns	29.253 ns	19.570 ns
Attenuation Rate	21.86%		35.34%		39.24%	

Table S4. Fitting parameters from the tri-exponential fit of the mapping-derived overall PL decays for nominally stoichiometric and PbI_2-modified $FA_{0.90}MA_{0.05}Cs_{0.05}PbI_3$ perovskite films before and after radiation exposure.

Condition	0% PbI_2 additive Film before Radiation	0% PbI_2 additive Film after Radiation	-5% PbI_2 additive Film before Radiation	-5% PbI_2 additive Film after Radiation	+5% PbI_2 additive Film before Radiation	+5% PbI_2 additive Film after Radiation
A_1	0.576	0.597	0.608	0.644	0.570	0.577
τ_1	0.987 ns	0.968 ns	0.924 ns	1.139 ns	1.018 ns	0.889 ns
A_2	0.308	0.301	0.307	0.295	0.325	0.307
τ_2	6.810 ns	6.234 ns	4.664 ns	5.752 ns	7.132 ns	6.010 ns
A_3	0.132	0.120	0.089	0.099	0.135	0.120
τ_3	40.964 ns	36.722 ns	18.724 ns	19.926 ns	41.916 ns	35.353 ns
τ_{avg}	29.310 ns	25.355 ns	10.504 ns	11.346 ns	29.684 ns	24.457 ns
Attenuation Rate	13.49%		-8.02%		17.61%	

Table S5. Fitting parameters from the tri-exponential fits of the mapping-derived overall PL decays for pristine and surface-treated $FA_{0.90}MA_{0.05}Cs_{0.05}PbI_3$ perovskite films before and after radiation exposure.

Condition	A_1	τ_1	A_2	τ_2	A_3	τ_3	τ_{avg}	Attenuation Rate
Pristine Film before Radiation	**0.576**	**0.987 ns**	**0.308**	**6.810 ns**	**0.132**	**40.964 ns**	**29.310 ns**	
Pristine Film after Radiation	**0.597**	**0.968 ns**	**0.301**	**6.234 ns**	**0.120**	**36.722 ns**	**25.355 ns**	**13.49%**
LAA Treated Film before Radiation	**0.646**	**1.187 ns**	**0.275**	**7.723 ns**	**0.115**	**45.147 ns**	**31.176 ns**	
LAA Treated Film after Radiation	**0.564**	**1.118 ns**	**0.315**	**7.788 ns**	**0.136**	**44.117 ns**	**31.322 ns**	**-0.47%**
DIA Treated Film before Radiation	**0.614**	**0.942 ns**	**0.301**	**5.666 ns**	**0.114**	**26.151 ns**	**16.735 ns**	
DIA Treated Film after Radiation	**0.641**	**0.886 ns**	**0.287**	**4.705 ns**	**0.104**	**20.194 ns**	**12.261 ns**	**26.74%**
Hydroquinone Treated Film before Radiation	**0.630**	**1.071 ns**	**0.289**	**6.885 ns**	**0.115**	**42.913 ns**	**29.797 ns**	
Hydroquinone Treated Film after Radiation	**0.641**	**1.076 ns**	**0.287**	**7.169 ns**	**0.111**	**43.581 ns**	**29.851 ns**	**-0.18%**
5MMBI Treated Film before Radiation	**0.633**	**1.144 ns**	**0.288**	**7.353 ns**	**0.116**	**44.940 ns**	**31.108 ns**	
5MMBI Treated Film after Radiation	**0.614**	**1.099 ns**	**0.294**	**7.470 ns**	**0.120**	**44.335 ns**	**30.900 ns**	**0.67%**
BCP Treated Film before Radiation	**0.675**	**1.019 ns**	**0.261**	**6.786 ns**	**0.106**	**41.367 ns**	**28.353 ns**	
BCP Treated Film after Radiation	**0.629**	**0.951 ns**	**0.277**	**6.501 ns**	**0.119**	**37.536 ns**	**26.189 ns**	**7.63%**

Table S6. Photovoltaic parameters of the devices with and without LAA treatment, before and after radiation exposure.

Sample	*J*sc (mA/cm^2)	*V*oc (V)	FF (%)	PCE (%)
LAA-Treated after Radiation	**23.45**	**1.079**	**77.87**	**19.71**
Pristine after Radiation	**22.52**	**1.036**	**73.05**	**17.04**
LAA-Treated before Radiation	**23.23**	**1.093**	**80.07**	**20.34**
Pristine before Radiation	**23.22**	**1.069**	**74.85**	**18.58**

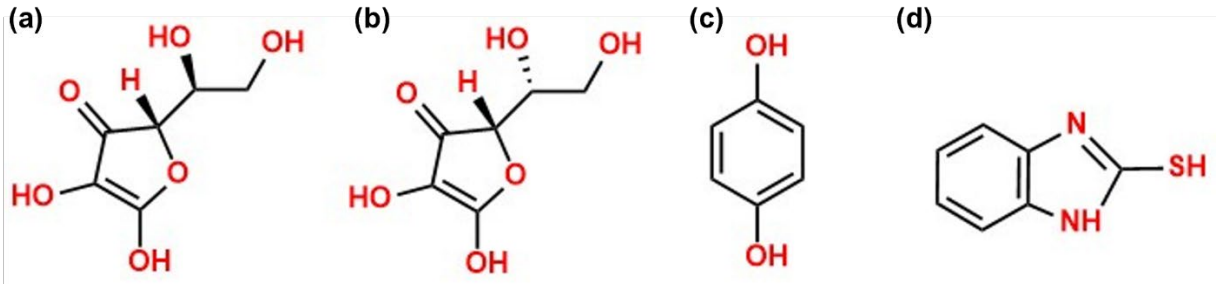

Figure S1. Chemical structure of (a) LAA (full name: L-Ascorbic acid), (b) DIA (full name: D-(−)-Isoascorbic acid), (c) Hydroquinone, and (d) 5MMBI (full name: 5-Methoxy-2-benzimidazolethiol).

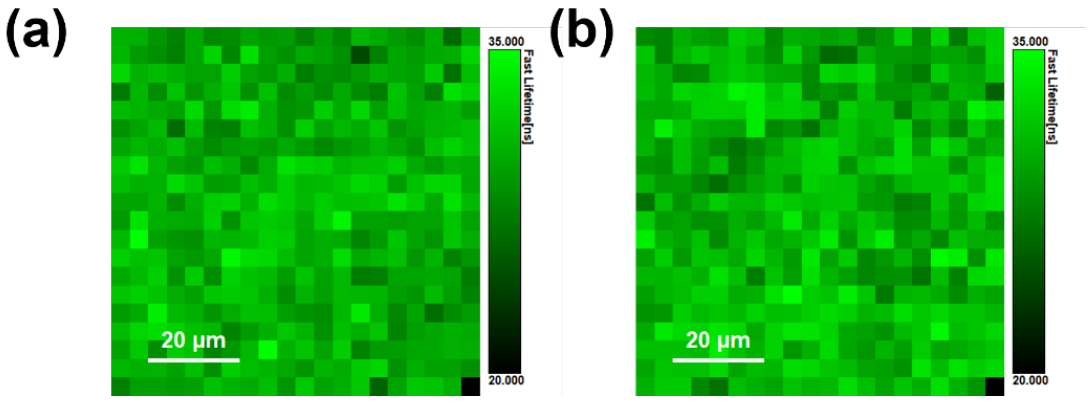

Figure S2. Experiment evaluating the effect of chlorobenzene washing on bare perovskite films without any evaporated upper layer. (a,b) Two-dimensional PL lifetime mapping images of the pristine perovskite film before and after chlorobenzene washing, respectively. The overall decay extracted from the 2D mapping measurements was used for the fitting summarized in Table S1. The average lifetime changes only slightly from 25.78 to 24.32 ns after washing, and the PL lifetime maps remain relatively uniform. This minor change is much weaker than the pronounced lifetime quenching observed after C_{60} or C_{60}/BCP/Ag evaporation followed by layer removal, indicating that the wash-and-peel-off recovery process itself is not the dominant origin of the interfacial lifetime loss observed in the main text.

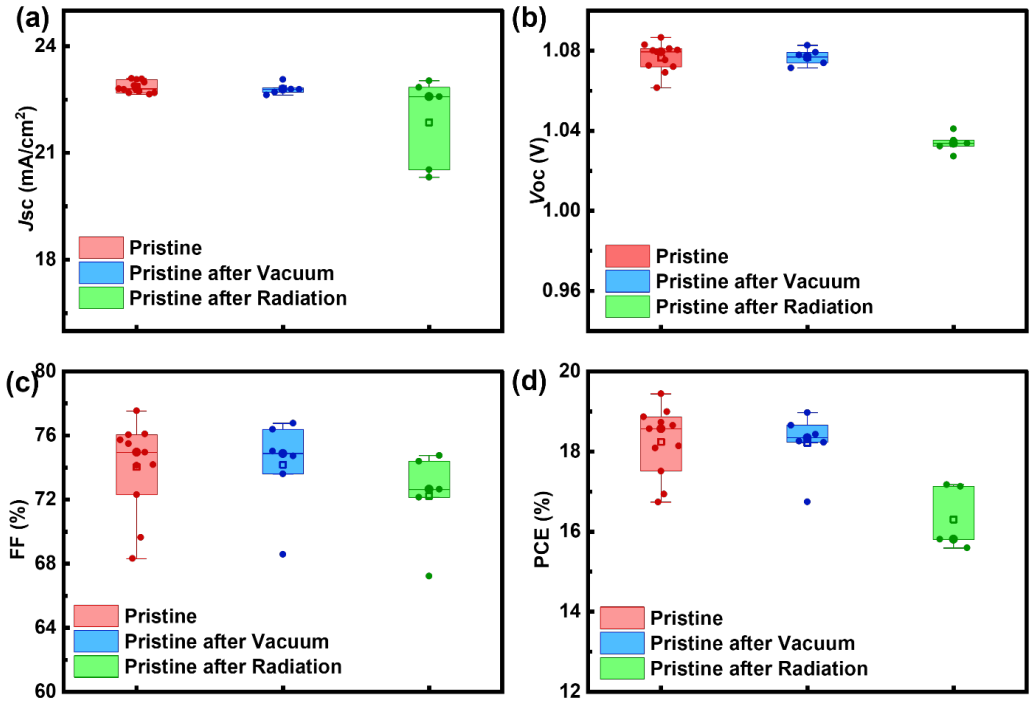

Figure S3. Statistical distribution of photovoltaic parameters for devices from three groups: untreated pristine film, pristine film in vacuum for 30 min, and pristine film under thermal radiation for 30 min. The parameters include PCE, V_{OC}, J_{SC}, and FF.

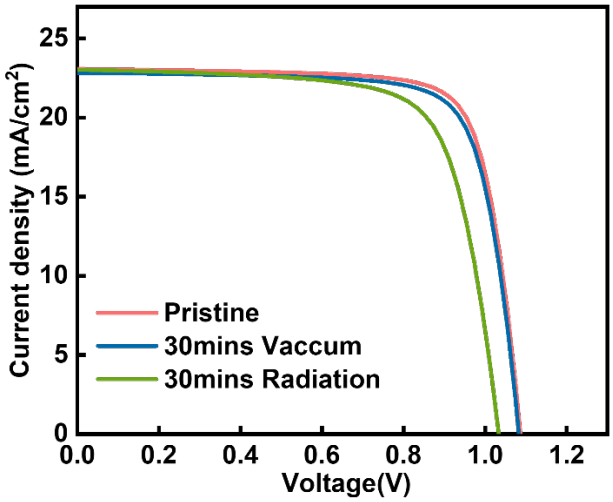

Figure S4. Champion *J–V* curves of devices from the three groups: untreated film, pristine film stored in vacuum for 30 min, and pristine film exposed to thermal radiation for 30 min.

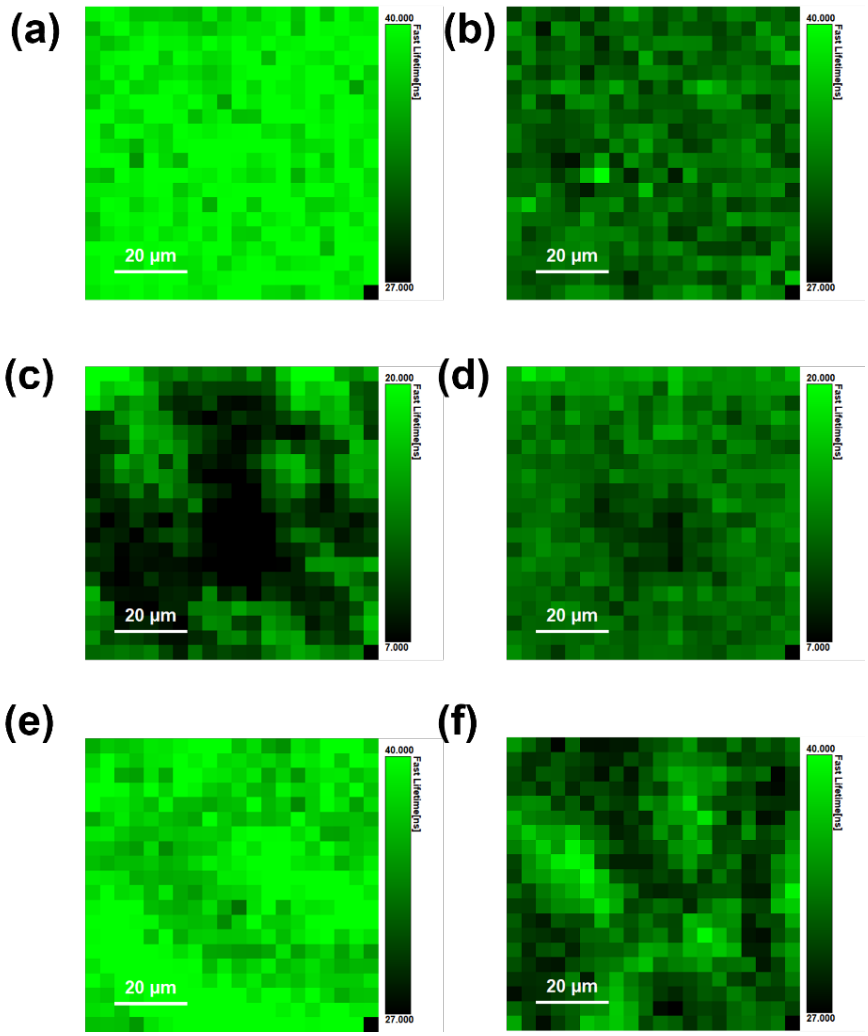

Figure S5. Stoichiometry-dependent two-dimensional PL lifetime mapping response of $FA_{0.90}MA_{0.05}Cs_{0.05}PbI_3$ perovskite films before and after 30 min thermal-radiation exposure. (a,b) Two-dimensional PL lifetime mapping images of the nominally stoichiometric perovskite film before and after radiation exposure, respectively. (c,d) Two-dimensional PL lifetime mapping images of the 5% PbI_2-deficient perovskite film before and after radiation exposure, respectively. (e,f) Two-dimensional PL lifetime mapping images of the 5% PbI_2-rich perovskite film before and after radiation exposure, respectively. The overall decay extracted from the 2D mapping measurements was used for the lifetime fitting summarized in Table S4. The nominal film shows a lifetime decrease from 29.310 to 25.355 ns, corresponding to 13.49% attenuation. The 5% PbI_2-rich film decreases from 29.684 to 24.457 ns, corresponding to 17.61% attenuation, indicating that a PbI_2-rich or iodide-rich near-surface environment remains susceptible to radiation-induced halide-loss chemistry. In contrast, the 5% PbI_2-deficient film exhibits a much shorter initial lifetime of 10.504 ns, indicating a more defective and recombination-limited starting condition. After radiation exposure, its 2D lifetime map becomes more spatially uniform and the fitted average lifetime slightly increases to 11.346 ns, corresponding to an apparent −8.02% attenuation. This

distinct response may indicate that radiation-induced iodine loss or halide redistribution partially equalizes the local recombination landscape in the initially iodine-deficient, highly heterogeneous film. However, this apparent lifetime increase should not be interpreted as beneficial passivation or improved radiation stability, because the absolute lifetime remains much lower than those of the nominal and PbI_2-rich films after radiation exposure. Therefore, the 5% PbI_2-deficient result is better described as radiation-induced homogenization of an initially heterogeneous recombination landscape, rather than true enhancement of film quality.

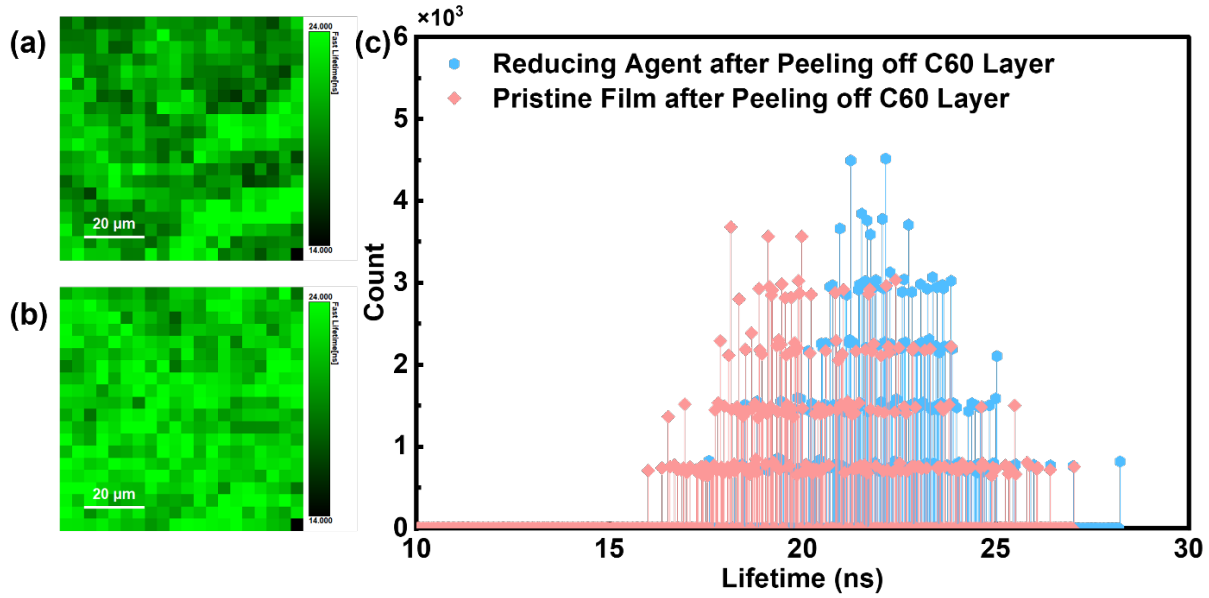

Figure S6. (a) 2D mapping of the average PL lifetime of the pristine perovskite film after removing the C_{60} layer. (b) 2D mapping of the average PL lifetime of the LAA-treated perovskite film after removing the C_{60} layer. (c) Corresponding histogram of the average PL lifetime distribution.

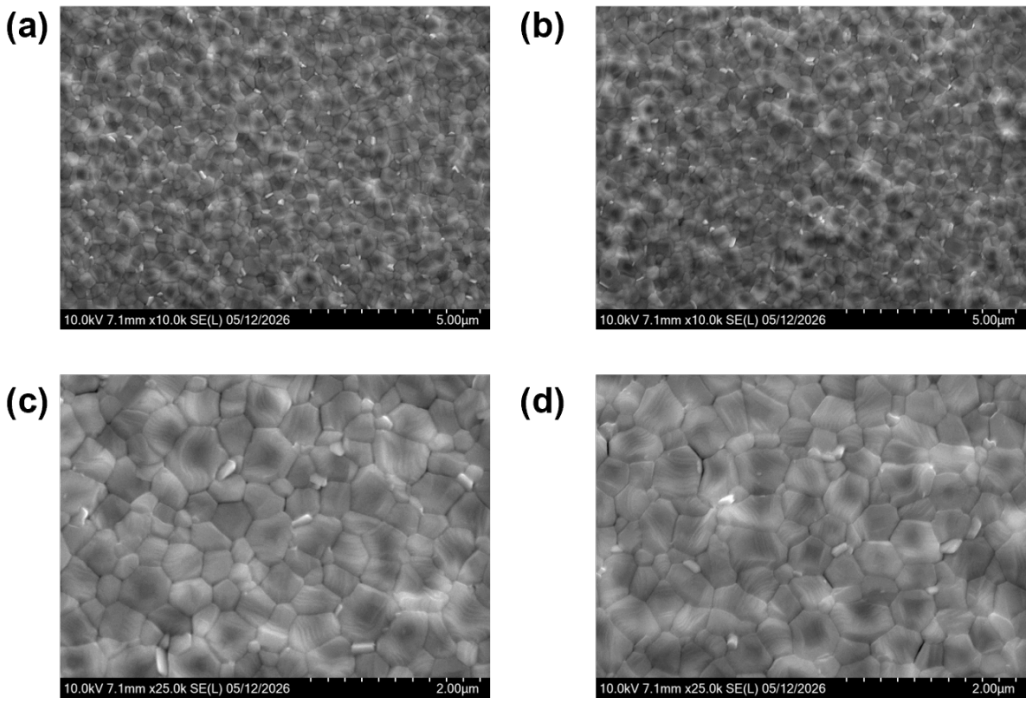

Figure S7. (a,c) Top-view SEM images of LAA-treated perovskite films before radiation exposure acquired at magnifications of 10k and 25k, respectively. (b,d) Top-view SEM images of LAA-treated perovskite films after radiation exposure acquired at magnifications of 10k and 25k, respectively. Before radiation, the LAA-treated film remains compact with clearly defined grains and limited nanoscale particulate surface features. After radiation, no obvious pinholes or severe grain-boundary widening are observed. The small particulates are not assigned to specific species without chemical mapping. Compared with untreated films, the LAA-treated films show suppressed grain-boundary-localized surface damage under thermal-radiation stress.

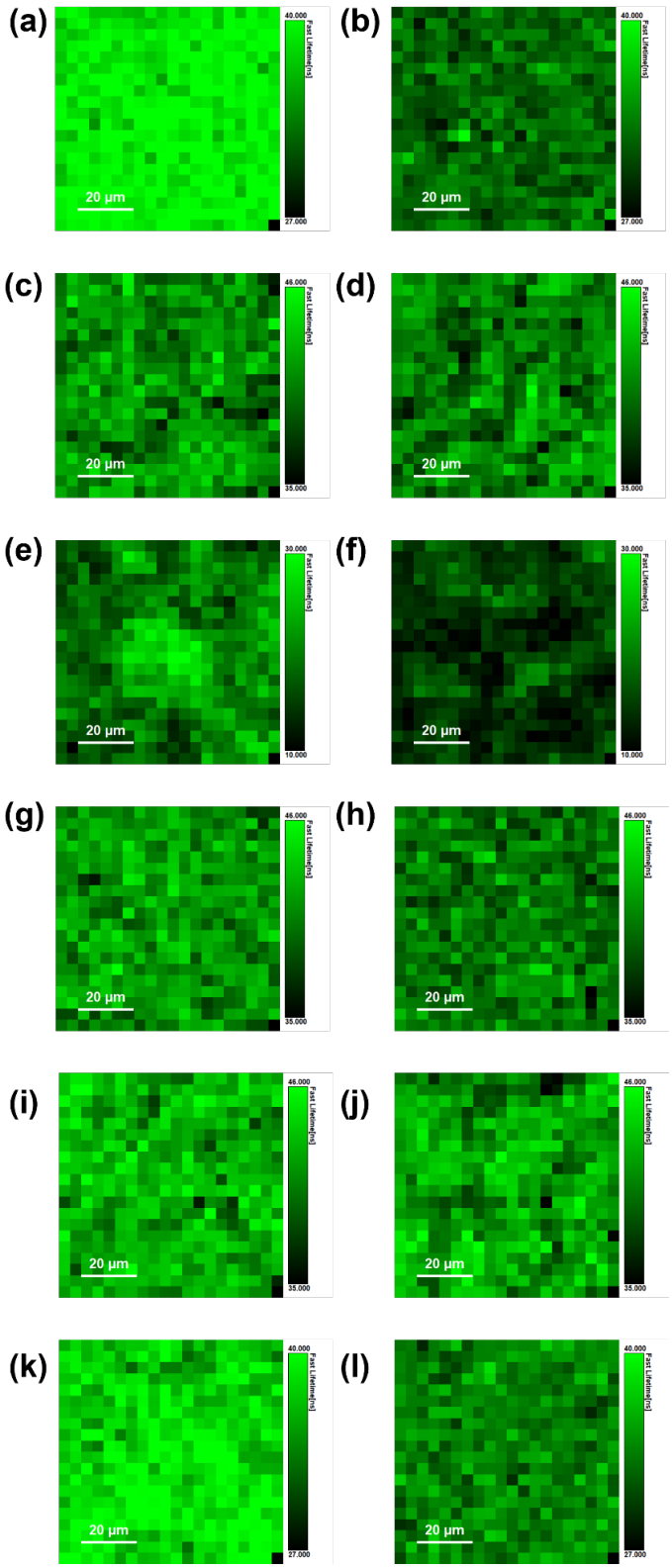

Figure S8. Comparison of the thermal-radiation response of pristine and surface-modified perovskite films based on two-dimensional PL lifetime mapping. (a,b) Pristine films before and

after radiation exposure, respectively. (c,d) LAA-treated films before and after radiation exposure, respectively. (e,f) DIA-treated films before and after radiation exposure, respectively. (g,h) Hydroquinone-treated films before and after radiation exposure, respectively. (i,j) 5MMBI-treated films before and after radiation exposure, respectively. (k,l) BCP-coated films before and after radiation exposure, respectively. The overall decay extracted from the 2D mapping measurements was used for the lifetime fitting summarized in Table S5. The pristine film decreases from 29.310 to 25.355 ns, corresponding to 13.49% attenuation. In contrast, the LAA-treated film essentially preserves its average lifetime after radiation exposure, changing from 31.176 to 31.322 ns, corresponding to an apparent −0.47% attenuation. Hydroquinone and 5MMBI also nearly preserve the average lifetime after radiation exposure, with attenuation values of −0.18% and 0.67%, respectively. In contrast, DIA shows substantial degradation, decreasing from 16.735 to 12.261 ns, corresponding to 26.74% attenuation. The BCP-coated control shows intermediate behavior, decreasing from 28.353 to 26.189 ns, corresponding to 7.63% attenuation. These results show that the protective effect is molecule-dependent and cannot be explained solely by physical overcoating. For clearer visualization of spatial contrast, the color scale bars of the 2D PL lifetime maps were adjusted individually; therefore, the apparent brightness should not be directly compared across different treatment groups.

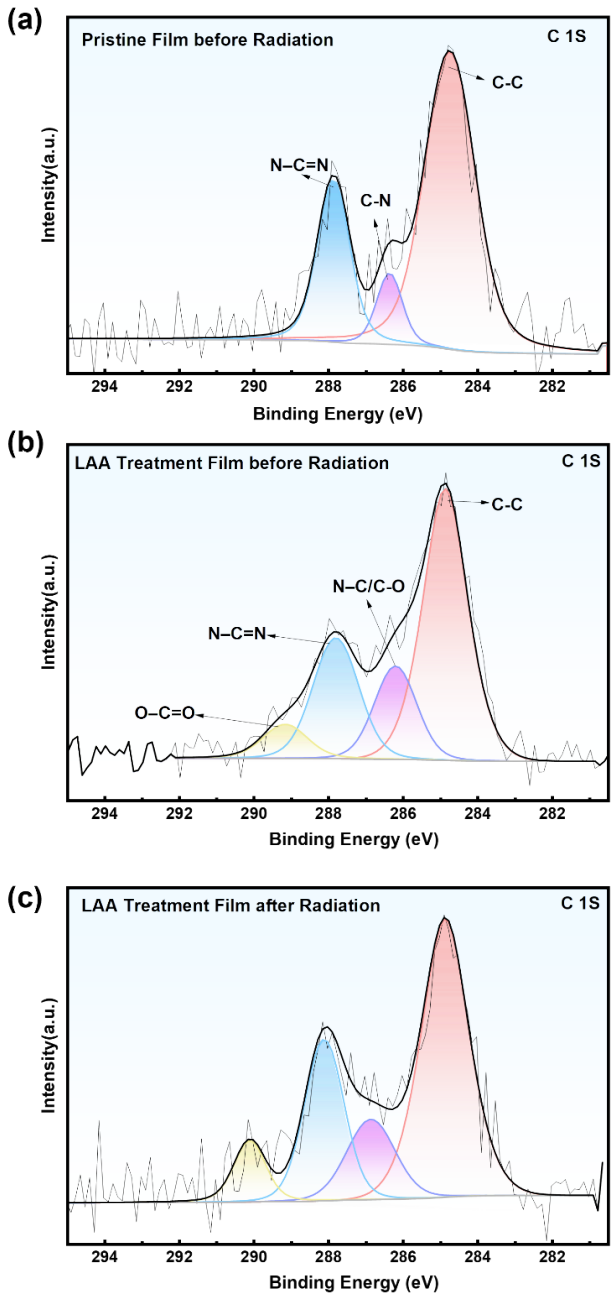

Figure S9. High-resolution C 1s XPS spectra of (a) pristine and (b, c) LAA-treated perovskite films before and after thermal-radiation exposure. The pristine perovskite film can be fitted mainly with components assigned to adventitious C–C/C–H, C–N/C–O, and FA-related N–C=N carbon environments, and no obvious high-binding-energy component near 289 eV is observed. After LAA treatment, an additional oxygenated-carbon feature appears at approximately 289.16 eV, together with enhanced intensity in the 286–288 eV region, indicating the presence of LAA-derived oxygenated carbon species at the surface. After thermal-radiation exposure, the oxygenated-carbon components in the LAA-treated film redistribute toward higher binding energy: the C–O/C–N-related component shifts from approximately 286.20 to 286.87 eV, the C=O/N–

C=N-related component shifts from approximately 287.81 to 288.12 eV, and the O–C=O/highly oxidized-carbon component shifts from approximately 289.16 to 290.11 eV. These spectral changes do not uniquely identify a specific molecular degradation product, but they provide chemical evidence that the LAA-derived surface layer evolves during irradiation, supporting the interpretation that LAA participates chemically in the protection process rather than acting only as an inert physical barrier.

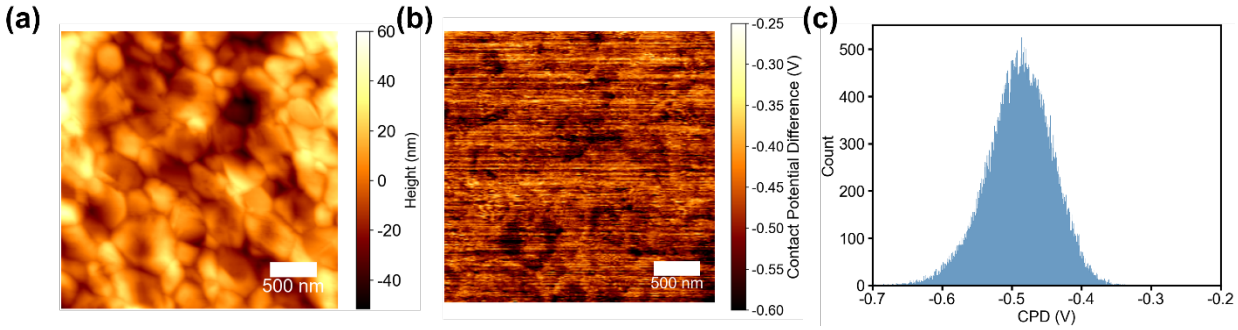

Figure S10. KPFM analysis of the LAA-treated perovskite film before thermal-radiation exposure. (a) AFM topography, (b) KPFM contact potential difference (CPD) map, and (c) the corresponding CPD distribution histogram of the fresh LAA-treated film.

Supplementary Note S1.

The baseline CPD of the fresh LAA-treated film is shifted negatively compared to the pristine, untreated perovskite. Notably, while L-ascorbic acid is a reducing agent, it does not induce a standard n-type doping effect (which would typically manifest as a positive CPD shift) prior to thermal exposure. This suggests that under mild processing conditions, the reducing agent does not possess sufficient activation energy to undergo spontaneous ground-state charge transfer with the perovskite lattice. Instead, the unreacted LAA molecules physically coordinate to the surface, where coordination-induced charge redistribution and the strong macroscopic dipole moment of their polar hydroxyl and carbonyl groups dominates the KPFM signal, inherently increasing the local measured work function.

However, the thermal radiation generated during vacuum evaporation provides the necessary activation energy to trigger the redox reaction. The LAA acts as a sacrificial reducing agent, reacting to suppress iodide oxidation. This chemical activation disrupts the initial molecular dipole layer, allowing the CPD to shift positively and return to a state that closely mirrors the preserved, pristine perovskite surface.

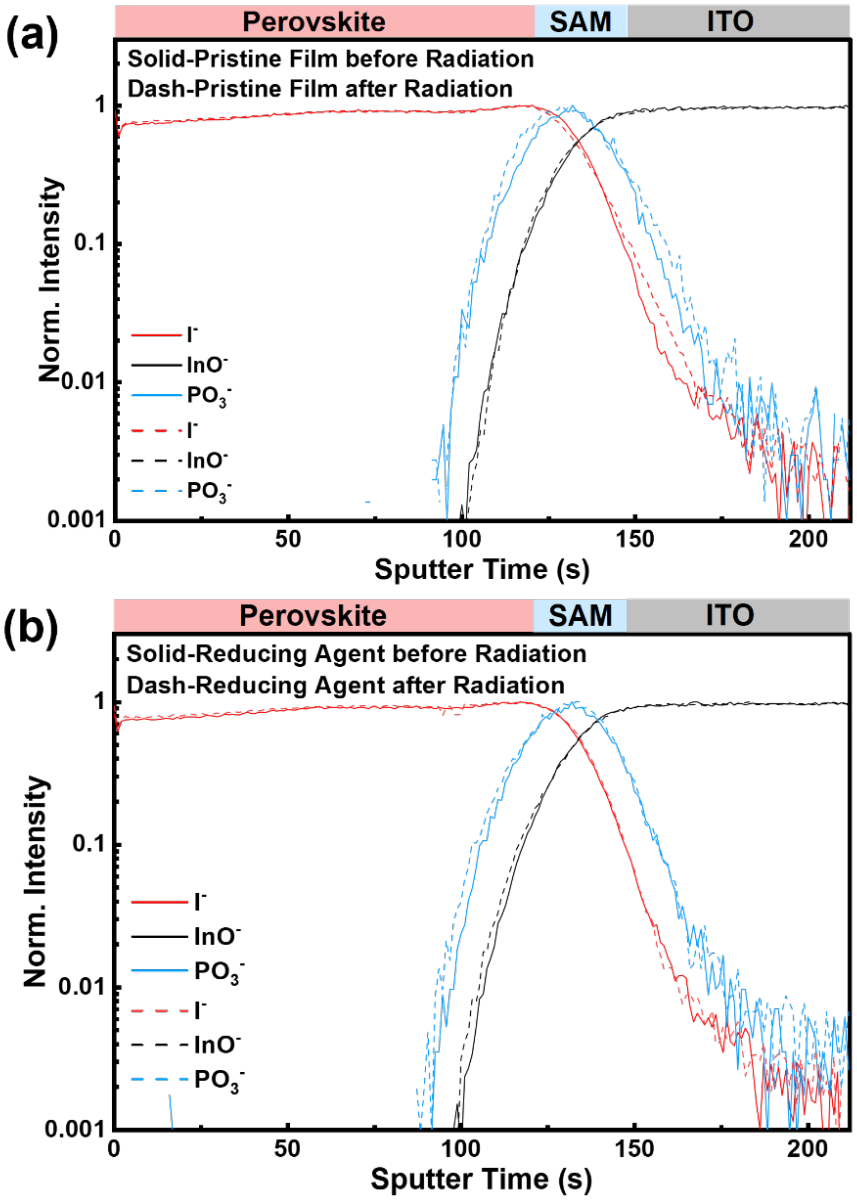

Figure S11. ToF-SIMS depth profiles across the perovskite/SAM/ITO stack. (a) Pristine sample before and after radiation. (b) Reducing agent-treated sample before and after radiation.

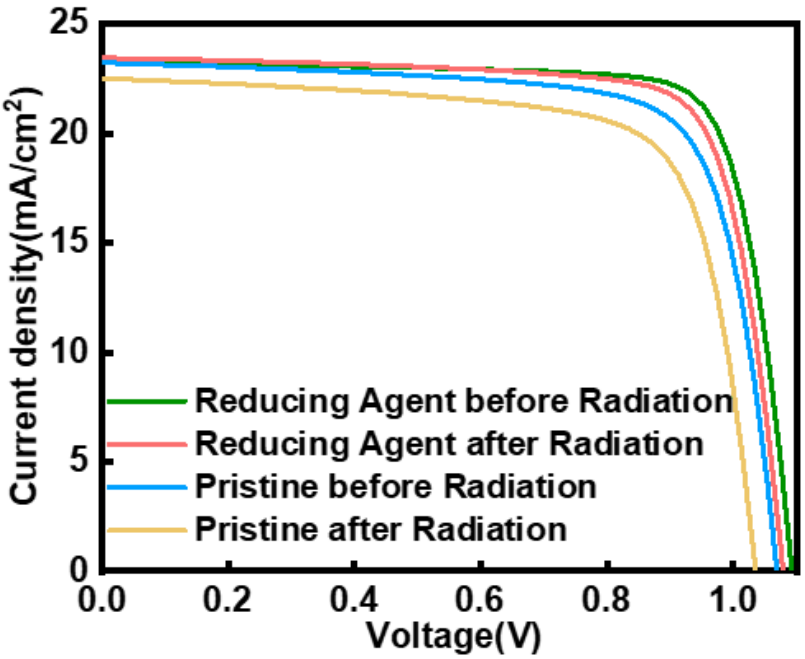

Figure S12. Champion current density-voltage (*J-V*) curves of pristine and reducing-agent-treated devices before and after radiation.

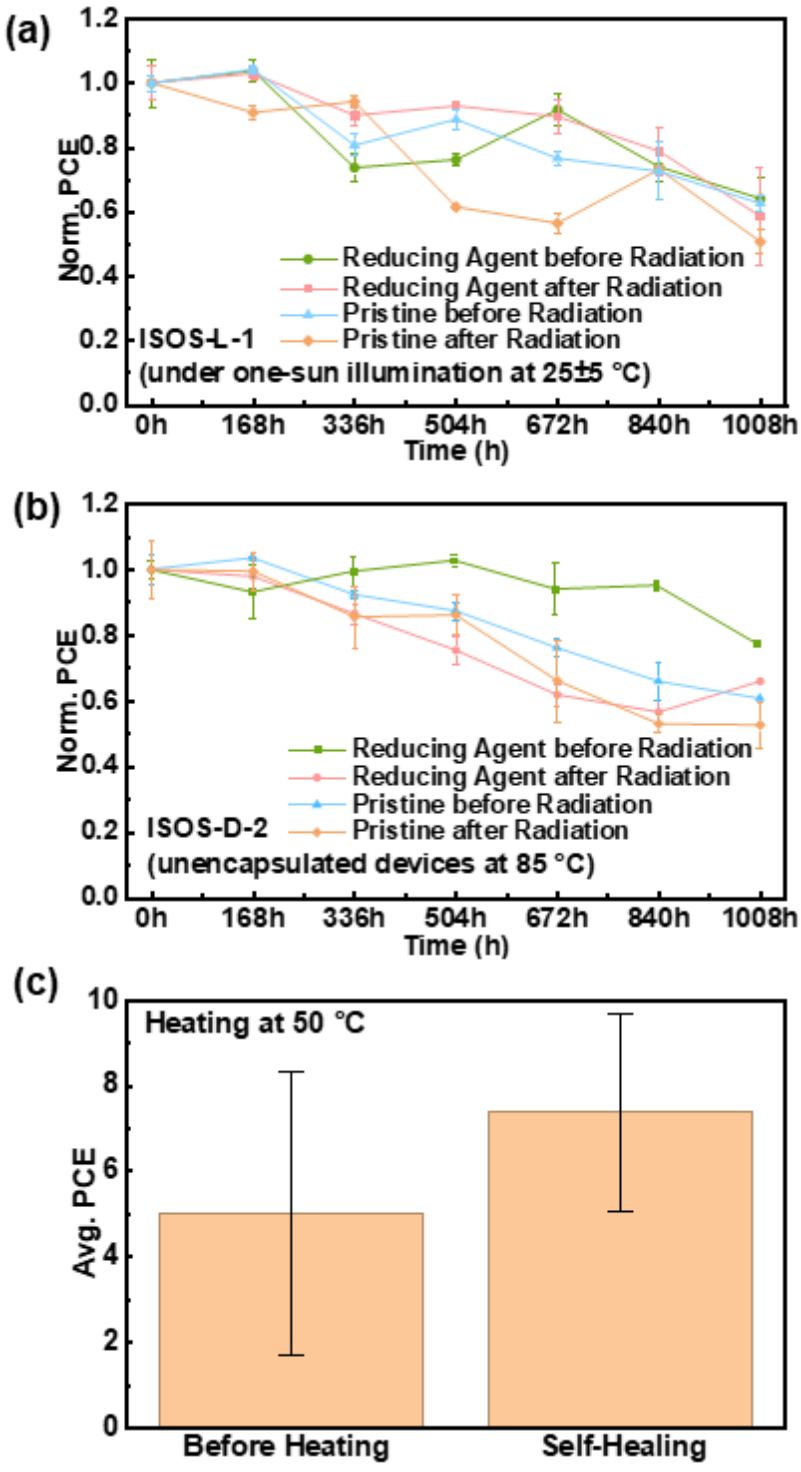

Figure S13. (a, b) Normalized PCE evolution of pristine and reducing-agent-treated devices before and after radiation over 1008 h under (**a**) ISOS-L-1 (light soaking under one-sun illumination at 25±5 °C) and (**b**) ISOS-D-2 (unencapsulated devices at 85 °C). **(c)** Average PCE values before and after mild thermal treatment at 50 °C, showing partial performance recovery.